

# Quark mean field model for nuclear matter and finite nuclei

H. Shen<sup>1</sup>

Department of Physics, Nankai University, Tianjin 300071, China

H. Toki<sup>2</sup>

Research Center for Nuclear Physics (RCNP), Osaka University, Ibaraki,  
Osaka 567-0047, Japan

## Abstract

We study nuclear matter and finite nuclei in terms of the quark mean field (QMF) model, in which we describe the nucleon using the constituent quark model. The meson mean fields, in particular the  $\sigma$  meson, created by other nucleons act on quarks inside a nucleon and change the nucleon properties in nuclear medium. The QMF model predicts an increasing size of the nucleon as well as a reduction of the nucleon mass in the nuclear environment. The present model is applied to study the properties of finite nuclei after fixing all the parameters by the nuclear matter properties, and it is found to give satisfactory results on the nuclear properties.

PACS numbers: 12.39.-x, 21.65.+f, 24.10.Jv, 24.85.+p

Keywords: quark mean field model, constituent quark model, nuclear matter, finite nuclei.

---

<sup>1</sup>e-mail address: shen@rcnp.osaka-u.ac.jp

<sup>2</sup>e-mail address: toki@rcnp.osaka-u.ac.jp

# 1 Introduction

We have been describing the nucleus with the assumption that the nucleon properties are unchanged from those of the free space nucleon. However, after the EMC effect was reported, we encounter often the discussions on the change of hadron properties in nuclei [1]. The EMC effect motivated many theoretical works on the study of hadrons in terms of quarks and gluons, although the pion interpretation is not excluded [2]. Among them, the QCD sum rule suggested a large change of the masses of the vector mesons and nucleons in nuclei [3]. It is very important to pursue these possibilities both theoretically and experimentally from various view points.

On the other hand, recent theoretical studies show that the properties of nuclear matter can be described nicely in terms of the relativistic Brueckner-Hartree-Fock (RBHF) approach [4]. With the nucleon-nucleon interaction fixed from the nucleon-nucleon scattering and the deuteron properties, we can reproduce very closely the nuclear matter saturation properties. The reason of the success is the large reduction of the nucleon effective mass in nuclear matter, which provides a density dependent repulsive contribution for the energy density. This reduction of the nucleon mass is also the source of the large spin-orbit splitting in finite nuclei, which is the key phenomenon of the nuclear shell model. Any model which changes the hadron properties in nuclear matter should respect these observations.

Guichon proposed an interesting model on the change of the nucleon properties in nuclear matter [5]. The model construction mimics the relativistic mean field theory, where the scalar and the vector meson fields couple not with nucleons but directly with the quarks in nucleons of the nuclei [6]. Hence, the nucleon properties change according to the strengths of the mean fields acting on the quarks. The nucleon is modeled in terms of the MIT bag model [7]. The scalar meson provides a strong attraction and as a consequence provides a negative mass to the quarks. The MIT bag model then reduces the nucleon mass in nuclear matter. This model was extended by Thomas and his collaborators under the name of the quark-meson coupling (QMC) model and applied to many observables [8].

The model of Guichon relies strongly on the choice of the nucleon model, for which the QMC model uses the MIT bag approach [7]. The MIT bag model assumes that the

inside of the bag is the perturbative vacuum and the quark mass is the bare mass, which is nearly zero for the up and down quarks. The perturbative vacuum has a larger energy than the non-perturbative vacuum and therefore the bag constant takes care of the energy difference between the two vacua. The non-perturbative objects as mesons are not allowed to exist in the bag interior and stay outside the bag. The chiral symmetry, the continuity of the axial current, requires the coupling of quarks with pions at the bag surface [9].

There are several conceptual problems to take the MIT bag model in the Guichon model;

1. The non-perturbative objects,  $\sigma$  and  $\omega$  mesons, have to be present in the perturbative vacuum.
2. The quark mass has to change from its bare mass due to the coupling to the  $\sigma$  meson.
3. For the up and down quarks, the resulting mass of the quarks is negative.

There may be some arguments to overcome the above mentioned points and justify the QMC model [8].

We would rather like to take another model for the nucleon, which is the constituent quark model [10]. In this model, the quarks get constituent quark masses due to spontaneous chiral symmetry breaking. It is then natural to have nearly zero mass pions as the Nambu-Goldstone bosons. Their coupling to the constituent quarks is provided by the chiral symmetry. This consideration makes a simple interpretation of the direct coupling of not only pions but also other mesons as  $\sigma$  and  $\omega$  mesons, since there is no boundary to separate the perturbative and the non-perturbative regions in this picture. The  $\sigma$  mean field could be considered as the amount related with the change of the chiral condensate in nuclear medium. Hence, it is natural to get the reduction of the quark mass in the nucleon inside of nuclei from the quark mass of the nucleon in the free space.

The constituent quark model is used extensively also for nucleon-nucleon interaction and later extended to baryon-baryon interactions in the SU(3) sector with great success [11, 12, 13, 14, 15, 16]. In this picture, it is natural that the mesons couple with quarks, since the nucleon is the composite of quarks.

Hence, it is very interesting to construct the Guichon model, where the nucleon is described in terms of constituent quarks, which couple with mesons and gluons. This model (we refer it as the quark mean field (QMF) model as named in Ref. [17].) has a direct

connection to the one-boson exchange model (Bonn potential). We expect, therefore, the quantitative results similar to those of the RBHF theory [4].

The paper is arranged as follows. In Section 2 we describe the concept of the QMF model and the procedure to perform calculations. In Section 3 we show the results for nuclear matter and in Section 4 the results for finite nuclei are presented. Section 5 is devoted to the summary of this paper.

## 2 Quark mean field model

We are still far away from describing nucleons and nuclei in terms of quarks and gluons using QCD. This difficulty arises from the fact that the theory becomes highly non-perturbative at low energy ( $p < 1\text{GeV}$ ). In addition, the QCD vacuum is realized in a non-trivial way, where the chiral symmetry is broken and the quarks and gluons are confined. The lattice QCD (LQCD) may handle hadrons. It is, however, too much to ask the LQCD to describe a system of many nucleons, the nuclei. Hence, we resort to an effective theory of QCD at low energy, which is based on QCD. The dual Ginzburg-Landau (DGL) theory may be a good candidate [18].

In this paper, we take a more phenomenological view point. We shall begin with a possible Lagrangian of the quark many body system. For this Lagrangian, we take into account the consequence of the non-perturbative gluon dynamics of spontaneous chiral symmetry breaking and quark confinement [19]. The effective Lagrangian of this level may be written as

$$\mathcal{L} = \bar{q} (i\gamma_\mu \partial^\mu - m_q - \chi_c - g\gamma_\mu A^\mu - g_i^q \phi_i \Gamma_i) q + \mathcal{L}(\chi_c, A_\mu, \phi_i). \quad (1)$$

Here,  $q$  denotes the quark fields with constituent quark mass  $m_q$ , which is of the order of  $300\text{MeV}$  to be consistent with the quark condensate and the pion decay constant [20]. The confinement is expressed in terms of  $\chi_c$ , which is given by the gluon dynamics [18]. The path from QCD to this expression is not yet known. One method might be the use of the dual Ginzburg-Landau (DGL) theory, which contains QCD monopoles in the Abelian space in the Abelian gauge and their condensation to induce the dual Meissner effect [18].  $A^\mu$  are the gluon fields with the running coupling constant  $g$  at the model scale. From the lattice QCD data, we find the effect of the gluon exchange interaction below  $r \leq 0.2\text{fm}$  and

hence the running coupling constant should be taken at the momentum scale,  $\mu \sim 1\text{GeV}$ . We include meson fields  $\phi_i$ , which couple with quark fields with the Dirac matrices  $\Gamma_i$  and the coupling strength  $g_i^q$ . The rest  $\mathcal{L}(\chi_c, A_\mu, \phi_i)$  denotes the confinement field, gluon and meson dynamics, which is not specified here explicitly. The explicit form is quite involved.

To proceed to many body system, we take the mean field approximation for the meson fields. We restrict to  $\sigma$ ,  $\omega$ , and  $\rho$  mesons, which are commonly used in the relativistic mean field model [6, 21, 22]. We note that in the mean field approximation, the pion field does not survive due to the spin average. Since quarks are confined completely in hadrons, we work out the many body problem in two steps. First, we construct the nucleon under the influence of the meson mean fields. Then in the second step, we solve the entire nuclear system with the change of the nucleon properties due to the presence of the mean fields, which is obtained in the first step.

The first step is to generate the nucleon system under the influence of the meson mean fields. In the constituent quark model, the quarks in a nucleon satisfies the following Dirac equation:

$$\left[ i\gamma_\mu \partial^\mu - m_q - \chi_c - g_\sigma^q \sigma(r) - g_\omega^q \omega(r) \gamma^0 - g_\rho^q \rho(r) \tau_3 \gamma^0 \right] q(r) = 0, \quad (2)$$

where  $\tau_3$  is the isospin matrix in our nuclear physics convention. Assuming the meson mean fields are constant within the small nucleon volume, we can then write the Dirac equation as

$$\left[ -i\vec{\alpha} \cdot \vec{\nabla} + \beta m_q^* + \beta \chi_c \right] q(r) = e^* q(r), \quad (3)$$

where  $m_q^* = m_q + g_\sigma^q \sigma$  and  $e^* = e - g_\omega^q \omega - g_\rho^q \rho \tau_3$ , with  $\sigma$ ,  $\omega$ , and  $\rho$  being the mean fields at the middle of the nucleon.  $e$  is the energy of the quark under the influence of the  $\sigma$ ,  $\omega$ , and  $\rho$  mean fields. The quark mass is modified to  $m_q^*$  due to the presence of the  $\sigma$  mean field. Here,  $g_\sigma^q$ ,  $g_\omega^q$ , and  $g_\rho^q$  are the coupling constants of the  $\sigma$ ,  $\omega$ , and  $\rho$  mesons with quarks, respectively. We take into account the spin correlations,  $E_{spin}$ , due to gluons and pions so that the mass difference between  $\Delta$  and nucleon arises. Hence, the nucleon energy is expressed as  $E_n^* = 3e^* + E_{spin}$ , where the vector contribution is removed here. There exists the spurious center of mass motion, which is removed in the standard method by  $M_n^* = \sqrt{E_n^{*2} - \langle p_{cm}^2 \rangle}$ , where  $\langle p_{cm}^2 \rangle = \sum_{i=1}^3 \langle p_i^2 \rangle$ , since the three constituent quarks are moving in the confining potential independently.

We now move to the second step, in which the nuclear many body system will be solved with the change of the nucleon properties obtained in the first step. We assume the following QMF Lagrangian,

$$\mathcal{L}_{QMF} = \bar{\psi} \left[ i\gamma_\mu \partial^\mu - M_n^* - g_\omega \omega \gamma^0 - g_\rho \rho \tau_3 \gamma^0 \right] \psi + \mathcal{L}_M(\sigma, \omega, \rho). \quad (4)$$

Here,  $\psi$  denotes the nucleon fields. The change of the nucleon properties is worked out in the first step and the outcome is exclusively expressed in  $M_n^*$ , which is a function of the quark mass correction,  $\delta m_q$ , related to the  $\sigma$  mean field as  $\delta m_q = -g_\sigma^q \sigma$ . The  $\omega$  and  $\rho$  mean fields do not cause any change of the nucleon properties [23], and they appear merely as the energy shift. These contributions are carried over as the nucleon-meson coupling terms with the replacement of the quark-meson couplings as  $g_\omega = 3g_\omega^q$  and  $g_\rho = g_\rho^q$ . We will apply the QMF model to study the properties of nuclear matter and finite nuclei in the following two Sections.

### 3 properties of nuclear matter

We calculate first the change of the nucleon properties as a function of the quark mass correction,  $\delta m_q$ , which is defined as  $\delta m_q = m_q - m_q^* = -g_\sigma^q \sigma$ . Here, the constituent quark mass is taken to be one third of the nucleon mass;  $m_q = M_n/3 = 313MeV$ . We take into account confinement in terms of the harmonic oscillator potential together with two Lorentz structures; (1) scalar potential  $\chi_c = \frac{1}{2}kr^2$  (2) scalar-vector potential  $\chi_c = \frac{1}{2}kr^2(1 + \gamma^0)/2$ . As pointed out in Ref. [24], the quark can not be confined when the vector potential is larger than the scalar one. Here, we just take two extreme types, since the Lorentz structure of the confinement is not established. As for the strength of the confining potential, we take  $k = 700$  and  $1000MeV/fm^2$ , in order to see the results depending on this factor. The spin correlation,  $E_{spin}$ , is fixed by the free nucleon mass as  $M_n = \sqrt{(3e + E_{spin})^2 - \langle p_{cm}^2 \rangle} = 939MeV$ . We assume further that the confining interaction and the spin correlations do not change in the nuclear medium.

We show in Fig.1 the results of the effective nucleon mass  $M_n^*$  as a function of  $\delta m_q$ . The results of the scalar potential with two oscillator parameters,  $k = 700$  and  $1000MeV/fm^2$ , are shown by the two solid curves. The effective nucleon mass decreases with  $\delta m_q$  and the curvature is clearly negative, which influences the nuclear matter properties, as will

be discussed soon. The results of the scalar-vector potential with the same two oscillator parameters are shown by the dashed curves. In this case the dependence of  $M_n^*$  on  $\delta m_q$  is almost linear as has been reported by Toki *et al.* [17]. We note that the results of the nuclear matter are very sensitive to the behavior of  $M_n^*$ .

To perform the nuclear matter calculation, we use the relativistic mean field (RMF) approximation containing nucleons, neutral scalar ( $\sigma$ ) and vector ( $\omega$ ) and isovector ( $\rho$ ) mesons. We need to specify the meson Lagrangian  $\mathcal{L}_M$ , since there are various versions of the meson Lagrangian in the RMF theory. The RMF theory with the TM1 parameter set includes the nonlinear terms both for  $\sigma$  and  $\omega$  mesons, which can reproduce the feature of the RBHF theory and satisfactory properties of finite nuclei [25]. In the present model, we would like to take the meson Lagrangian as

$$\begin{aligned}\mathcal{L}_M = & \frac{1}{2}(\partial_\mu\sigma)^2 - \frac{1}{2}m_\sigma^2\sigma^2 - \frac{1}{4}g_3\sigma^4 \\ & - \frac{1}{4}(\partial_\mu\omega_\nu - \partial_\nu\omega_\mu)^2 + \frac{1}{2}m_\omega^2\omega_\mu^2 + \frac{1}{4}c_3\omega_\mu^4 \\ & - \frac{1}{4}(\partial_\mu\rho_\nu^a - \partial_\nu\rho_\mu^a)^2 + \frac{1}{2}m_\rho^2(\rho_\mu^a)^2.\end{aligned}\tag{5}$$

Comparing with the Lagrangian in the RMF(TM1) model [25], we have deleted the nonlinear term  $\frac{1}{3}g_2\sigma^3$ , so that less free parameters are contained in the present model. Actually, the nonlinear term  $\frac{1}{3}g_2\sigma^3$  plays similar role as the nonlinear term  $\frac{1}{4}g_3\sigma^4$ . Note that we have dropped the  $\rho_\mu^a \times \rho_\nu^b$  term, since this term vanishes at the mean field level. Now, the nucleons and mesons obey the Euler-Lagrange equations derived from the QMF Lagrangian, which can be written, for the nuclear matter, as

$$\left[i\gamma_\mu\partial^\mu - M_n^* - g_\omega\omega\gamma^0 - g_\rho\rho\tau_3\gamma^0\right]\psi = 0,\tag{6}$$

$$m_\sigma^2\sigma + g_3\sigma^3 = -\frac{\partial M_n^*}{\partial\sigma}\langle\bar{\psi}\psi\rangle,\tag{7}$$

$$m_\omega^2\omega + c_3\omega^3 = g_\omega\langle\bar{\psi}\gamma^0\psi\rangle,\tag{8}$$

$$m_\rho^2\rho = g_\rho\langle\bar{\psi}\tau_3\gamma^0\psi\rangle.\tag{9}$$

Here, the bracket  $\langle \rangle$  means the expectation value of the operator between the nuclear ground state. For the  $\omega$  and  $\rho$  parts we have replaced the quark-meson couplings  $g_i^q$  by the nucleon-meson couplings  $g_i$  as  $g_\omega = 3g_\omega^q$  and  $g_\rho = g_\rho^q$ . The effective mass  $M_n^*$

and its derivative with respect to the  $\sigma$  mean field,  $\partial M_n^*/\partial\sigma$ , are not trivial functions of the  $\sigma$  mean field, because  $M_n^*$  depends on  $\delta m_q = -g_\sigma^q\sigma$  non-trivially as shown in Fig.1. Comparing with the RMF theory, the  $\partial M_n^*/\partial\sigma$  in the QMF model is equal to the  $g_\sigma$  in the RMF model. We show in Fig.2 the quantities  $g_\sigma(\sigma)/g_\sigma(0)$  as a function of  $\delta m_q$ . In the case of the scalar-vector potential, the dependence of  $g_\sigma(\sigma)$  on  $\delta m_q$  is very small. On the other hand, in the case of the scalar potential,  $g_\sigma(\sigma)$  increases rapidly with  $\delta m_q$ .

In the present model, there are five free parameters,  $g_\sigma^q$ ,  $g_\omega^q$ ,  $g_3$ ,  $c_3$ , and  $g_\rho$ , which need to be determined. We would like to follow the method in Ref. [26] to determine these parameters. We determine these five parameters by reproducing five equilibrium properties of nuclear matter [25, 26]. The equilibrium properties used here are listed in Table 1. As for the other parameters, we take  $m_\omega = 783\text{MeV}$  and  $m_\rho = 770\text{MeV}$ . We note that the variation of  $m_\sigma$  at fixed  $g_\sigma^q/m_\sigma$  and  $g_3/m_\sigma^4$  has no effect on the nuclear matter properties, but the  $\sigma$  meson mass determines the range of the attractive interaction and affects the nuclear surface slope and its thickness for finite nuclei and hence the finite nuclear properties. The mass of the  $\sigma$  meson is chosen to reproduce the charge radius of  $^{40}\text{Ca}$  to be around  $3.45\text{fm}$ . The parameter sets for the four cases used in the present model are given in Table 2.

Using the parameters given in table 2, the nuclear matter properties can be obtained by solving the above Euler-Lagrange equations self-consistently. We plot in Fig.3 the energy per nucleon,  $E/A$ , as functions of the nuclear matter density  $\rho$ . In Fig.4, we plot the scalar potential,  $U_S$ , and the vector potentials,  $U_V$ , as functions of density  $\rho$ . The results in the RMF(TM1) model are also shown for comparison. Definitely the results at  $\rho = \rho_0 = 0.145\text{fm}^{-3}$  do not change due to the construction of the parameter sets, but the results at different densities depend somewhat on the parameter set.

Since the QMF model uses the constituent quark model to describe the nucleon in medium, the nucleon properties change according to the strengths of the mean fields. We plot the ratio of the nucleon rms radius in medium to that in free space as a function of density in Fig.5. All of the four curves show the increase of the nucleon radius in medium. The nucleon radius increases by about  $5\% \sim 9\%$  at the normal matter density for different confinement parameters and the type of the potential. It would be very interesting to calculate the EMC effect with the change of the nucleon properties, in



particular, with the increase of the nucleon radius. If we make a comparison with the QMC model of Thomas and his collaborators [8], a significantly swollen nucleon radius is predicted in the present QMF model without adding extra parameters, while almost no swelling is found in the original QMC model when the bag constant does not depend on density [8]. We note here that there are a few modified versions of the QMC model, which could reproduce the swollen nucleon radius by changing the bag constant [26].

## 4 Properties of finite nuclei

To study the properties of finite nuclei, the electromagnetic field must also be included, which does not appear in infinite nuclear matter. The construction of the nucleon inside nuclei will be rather complicated if the variation of the meson mean fields over the nucleon volume is considered. We have to take some suitably averaged form for the meson mean fields in order to make the numerical solution feasible. Here, we use the local density approximation, which replace the meson mean fields at the quark level by their value at the center of the nucleon and neglect the spatial variation of the mean fields over the small nucleon volume. If we restrict our consideration to spherically symmetric nuclei, the Euler-Lagrange equations are then written as

$$\left[ i\gamma_\mu \partial^\mu - M_n^* - g_\omega \omega(r) \gamma^0 - g_\rho \rho(r) \tau_3 \gamma^0 - e \frac{(1 - \tau_3)}{2} A(r) \gamma^0 \right] \psi = 0, \quad (10)$$

$$\Delta \sigma(r) - m_\sigma^2 \sigma(r) - g_3 \sigma^3(r) = \frac{\partial M_n^*}{\partial \sigma} \langle \bar{\psi} \psi \rangle, \quad (11)$$

$$\Delta \omega(r) - m_\omega^2 \omega(r) - c_3 \omega^3(r) = -g_\omega \langle \bar{\psi} \gamma^0 \psi \rangle, \quad (12)$$

$$\Delta \rho(r) - m_\rho^2 \rho(r) = -g_\rho \langle \bar{\psi} \tau_3 \gamma^0 \psi \rangle, \quad (13)$$

$$\Delta A(r) = -e \langle \bar{\psi} \frac{(1 - \tau_3)}{2} \gamma^0 \psi \rangle. \quad (14)$$

Here, the meson mean fields are functions of  $r$ , which is the radial coordinate of the nucleon center. The meson mean fields are approximated to be constants over the small nucleon volume. We solve the above equations self-consistently with the amount of  $M_n^*$  and  $\partial M_n^* / \partial \sigma$  obtained in the first step.

We take the same coupling constants and meson masses as used in nuclear matter to study the properties of finite nuclei. We follow some prescriptions in Ref. [25] to deal with the center-of-mass corrections and the pair corrections. The charge densities and the rms charge radii are calculated by convoluting the point nucleon density with an empirical nucleon form factor as in Ref [25]. The calculated results for the binding energies per nucleon  $E/A$  and the rms charge radii  $R_c$  are compared with experimental values in Table 3. For the case of the scalar-vector potential, the calculated results for  $E/A$  and  $R_c$  are almost same as the RMF(TM1) results. This is because the derivative  $\partial M_n^*/\partial\sigma$  is almost unchanged with the  $\sigma$  mean field as shown in Fig.2. On the other hand, for the case of the scalar potential,  $E/A$  are somewhat underestimated. This is caused by the increase of  $g_\sigma$  with the  $\sigma$  mean field as shown in Fig.2. We need, instead, the decrease of the effective  $g_\sigma$  in order to achieve good results. In Table 4, the calculated spin-orbit splittings for  $^{40}\text{Ca}$  and  $^{208}\text{Pb}$  are presented. The results are similar to those of the RMF(TM1). This is due to the fact that the effective mass was used to obtain the coupling constants. In Fig.6 we show calculated charge density distributions for  $^{40}\text{Ca}$  in the QMF model and compare with the experimental distribution [27] and the results in the RMF(TM1) model. Even though there are still some discrepancies between the results in the QMF model and the experimental values, we consider the QMF model provides reasonable results for finite nuclei.

## 5 Conclusion

We have developed the quark mean field (QMF) model to describe the change of nucleon properties in nuclei and at the same time the properties of nuclear matter and finite nuclei. We have used the constituent quark model for the nucleon, which naturally allows the direct coupling of  $\sigma$ ,  $\omega$ , and  $\rho$  mesons with quarks. The mean field Lagrangian at the nucleon level reflects the direct coupling of mesons with quarks merely through the appearance of the effective nucleon mass, which is a function of the  $\sigma$  mean field. With our model setting and our parameter choices, we can perform the numerical calculations for nuclear matter and finite nuclei.

We have investigated the QMF model with different types of the confinement potential.

We have taken the mean field Lagrangian with nonlinear terms for both  $\sigma$  and  $\omega$  mesons. The comparison between the QMF model and the RMF(TM1) model has been done. The QMF model can provides a significantly swollen nucleon radius in nuclear medium. At the normal matter density, the nucleon radius increases by about  $5\% \sim 9\%$ . We calculate also the properties of finite nuclei, the resulting binding energies per nucleon  $E/A$  and charge radii  $R_c$  are close to the experimental values, as well as the spin-orbit splittings in the QMF model are also satisfactory.

## Acknowledgments

H. Shen would like to thank A. Hosaka for fruitful discussions and helpful suggestions. This work was supported in part by National Natural Science Foundation of China.

# References

- [1] EMC, J.J. Aubert *et al.*, Phys. Lett. **123B**, 275 (1983).
- [2] M. Ericson and A.W. Thomas, Phys. Lett. **128B**, 112 (1983).
- [3] T. Hatsuda, Journal of Korean Phys. Soc. **29**, 291 (1996).
- [4] R. Brockmann and R. Machleidt, Phys. Rev. **C42**, 1965 (1990).
- [5] P. Guichon, Phys. Lett. **B200**, 235 (1988).
- [6] B.D. Serot and J.D. Walecka, Adv. Nucl. Phys. **16**, 1 (1986).
- [7] T.De. Grand, R.L. Jaffe, K. Johnson, and J. Kiskis, Phys. Rev. **D12**, 2060 (1975).
- [8] K. Saito, A. Michels, and A.W. Thomas, Phys. Rev **C46**, R2149 (1992);  
K. Saito and A.W. Thomas, Nucl. Phys. **A574**, 659 (1994);  
K. Saito and A.W. Thomas, Phys. Rev. **C51**, 2757 (1995);  
P. Guichon, K. Saito, E. Rodionov, and A. W. Thomas, Nucl. Phys. **A601**, 349 (1996).
- [9] A. Hosaka and H. Toki, Phys. Rep. **277**, 65 (1997).
- [10] N. Isgur and G. Karl, Phys. Rev. **D18**, 4187 (1978).
- [11] H. Toki, Z. Physik **A294**, 173 (1980).
- [12] M. Oka and K. Yazaki, Phys. Lett. **B90**, 41 (1980).
- [13] A. Faessler, F. Fernandez, G Luebeck, and K. Shimizu, Phys. Lett. **112B**, 201 (1982);  
A. Faessler, F. Fernandez, G Luebeck, and K. Shimizu, Nucl. Phys. **A402**, 555 (1983).
- [14] Y. Fujiwara, C. Nakamoto, and Y. Suzuki, Phys. Rev. Lett. **76**, 2242 (1996).
- [15] U. Straub, Z.Y. Zhang, K. Bräuer, A. Faessler, S.B. Khadkikar, and G. Lübeck, Nucl.Phys. **A483**, 686 (1988).
- [16] A. Faessler and U. Straub, Phys. Lett. **B183**, 10 (1987).
- [17] H. Toki, U. Meyer, A. Faessler, and R. Brockmann, Phys. Rev. **C58**, 3749 (1998).
- [18] H. Suganuma, S. Sasaki, and H. Toki, Nucl. Phys. **B435**, 207 (1995);  
H. Toki, H. Suganuma, and S. Sasaki, Nucl. Phys. **A577**, 353c (1994).
- [19] T. Chen and L. Li, "Gauge Theory of Elementary Particle Physics", Oxford Science Pub. (1986).

- [20] U. Vogl and W. Weise, Prog. Part. Nucl. Phys. **27**, 195 (1991);  
T. Hatsuda and T. Kunihiro, Phys. Rep. **247**, 221 (1994).
- [21] D. Hirata, H. Toki, T. Watabe, I. Tanihata, and B. V. Carlson, Phys. Rev. **C44**, 1467 (1991).
- [22] Y. K. Gambhir, P. Ring, and A. Thimet, Ann. of Phys. **198**, 132 (1990).
- [23] S. Fleck, W. Bentz, K. Shimizu, and K. Yazaki, Nucl. Phys. **A510**, 731 (1990).
- [24] Y. Shibata and H. Tezuka, Z. Phys. **C62**, 533 (1994).
- [25] Y. Sugahara and H. Toki, Nucl. Phys. **A579**, 557 (1994).
- [26] H. Muller and B. K. Jennings, Nucl. Phys. **A640**, 55 (1998).
- [27] H. de Vries, C. W. de Jager and C. de Vries, Atomic Data and Nuclear Data Tables **36**, 495 (1987).
- [28] X. Campi and D. W. Sprung, Nucl. Phys. **A194**, 401 (1972).

## Figure captions

**Figure 1:** The effective nucleon mass  $M_n^*$  as functions of the quark mass correction  $\delta m_q$ .

The results in the QMF model with  $\chi_c = \frac{1}{2}kr^2$  are shown by solid curves, while those with  $\chi_c = \frac{1}{2}kr^2(1 + \gamma^0)/2$  are shown by dashed curves. For each potential shown are the two results for two confining strengths.

**Figure 2:** The ratios of the  $\sigma$ -nucleon coupling in medium,  $g_\sigma(\sigma) = \partial M_n^*/\partial\sigma$ , to that in free space,  $g_\sigma(0)$ , as functions of the quark mass correction  $\delta m_q$ .  $\delta m_q$  is connected with the  $\sigma$  mean field as  $\delta m_q = -g_\sigma^q\sigma$ . The curves are labeled as in Fig.1.

**Figure 3:** The energy per nucleon,  $E/A$ , as functions of the nuclear matter density  $\rho$ .

The results in the QMF model with  $\chi_c = \frac{1}{2}kr^2$  are shown by solid curves, while those with  $\chi_c = \frac{1}{2}kr^2(1 + \gamma^0)/2$  are shown by dashed curves with  $k = 700$ . The results in the RMF(TM1) model are plotted by dotted curves for comparison.

**Figure 4:** The scalar potential,  $U_S$ , and the vector potential,  $U_V$ , as functions of the nuclear matter density  $\rho$ . The curves are labeled as in Fig.3.

**Figure 5:** The ratios of the nucleon rms radius  $R$  to that in free space  $R_0$  as functions of the nuclear matter density  $\rho$ . The curves are labeled as in Fig.1.

**Figure 6:** The charge density distributions for  $^{40}\text{Ca}$  compared with the experimental data (solid curve) [27]. The dash-dotted and dashed curves are the results in the QMF model with  $\chi_c = \frac{1}{2}kr^2$  ( $k = 700$ ) and  $\chi_c = \frac{1}{2}kr^2(1 + \gamma^0)/2$  ( $k = 700$ ), respectively. The results in the RMF(TM1) model are plotted by dotted curves for comparison.

Table 1: The nuclear matter properties used to determine the five free parameters in the present model. The saturation density and the energy per particle are denoted by  $\rho_0$  and  $E/A$ , and the incompressibility by  $k$ , the effective mass by  $M_n^*$  and the symmetry energy by  $a_{sym}$ .

$\rho_0$ ( $fm^{-3}$ )	$E/A$ ( $MeV$ )	$k$ ( $MeV$ )	$M_n^*/M_n$	$a_{sym}$ ( $MeV$ )
0.145	-16.3	280	0.63	35

Table 2: The parameters in the QMF model are listed. For comparison, the parameters in the RMF(TM1) model are also presented.

Model		$g_\sigma^q$	$g_\omega^q$	$g_2$ ( $fm^{-1}$ )	$g_3$	$c_3$	$g_\rho$	$m_\sigma$ ( $MeV$ )
QMF	$k = 700$	3.14	4.20	0	50.7	53.6	4.3	470
$\chi_c = \frac{1}{2}kr^2$	$k = 1000$	2.98	4.17	0	52.8	36.4	4.3	460
QMF	$k = 700$	4.18	4.42	0	36.8	214	4.3	515
$\chi_c = \frac{1}{2}kr^2(1 + \gamma^0)/2$	$k = 1000$	4.11	4.38	0	36.4	167	4.3	510
RMF (TM1)		$g_\sigma = 10.029$	$g_\omega = 12.614$	-7.2325	0.6183	71.308	4.6322	511.2

Table 3: The binding energies per nucleon  $E/A$  and the rms charge radii  $R_c$  in the present model compared with the results in the RMF(TM1) model and the experimental values [25].

Model		$E/A$ (MeV)				$R_c$ (fm)			
		$^{40}Ca$	$^{48}Ca$	$^{90}Zr$	$^{208}Pb$	$^{40}Ca$	$^{48}Ca$	$^{90}Zr$	$^{208}Pb$
QMF	$k = 700$	7.53	7.66	7.92	7.36	3.45	3.46	4.28	5.53
$\chi_c = \frac{1}{2}kr^2$	$k = 1000$	7.32	7.46	7.75	7.24	3.45	3.46	4.28	5.53
QMF	$k = 700$	8.35	8.43	8.54	7.81	3.44	3.46	4.28	5.54
$\chi_c = \frac{1}{2}kr^2(1 + \gamma^0)/2$	$k = 1000$	8.21	8.30	8.43	7.73	3.44	3.46	4.27	5.53
RMF (TM1)		8.62	8.65	8.71	7.87	3.44	3.45	4.27	5.53
Exp.		8.55	8.67	8.71	7.87	3.45	3.45	4.26	5.50

Table 4: The spin-orbit splittings for  $^{40}Ca$  and  $^{208}Pb$  in the present model compared with the results in the RMF(TM1) model and the experimental values [28]. All quantities are in MeV.

Model		$^{40}Ca$		$^{208}Pb$	
		Proton	Neutron	Proton	Neutron
		$(1d_{5/2} - 1d_{3/2})$	$(1d_{5/2} - 1d_{3/2})$	$(1g_{9/2} - 1g_{7/2})$	$(2f_{7/2} - 2f_{5/2})$
QMF	$k = 700$	-5.8	-5.9	-3.5	-1.8
$\chi_c = \frac{1}{2}kr^2$	$k = 1000$	-5.8	-5.8	-3.5	-1.8
QMF	$k = 700$	-5.6	-5.6	-3.3	-1.9
$\chi_c = \frac{1}{2}kr^2(1 + \gamma^0)/2$	$k = 1000$	-5.7	-5.8	-3.4	-1.9
RMF (TM1)		-5.7	-5.7	-3.4	-1.8
Exp.		-7.2	-6.3	-4.0	-1.8



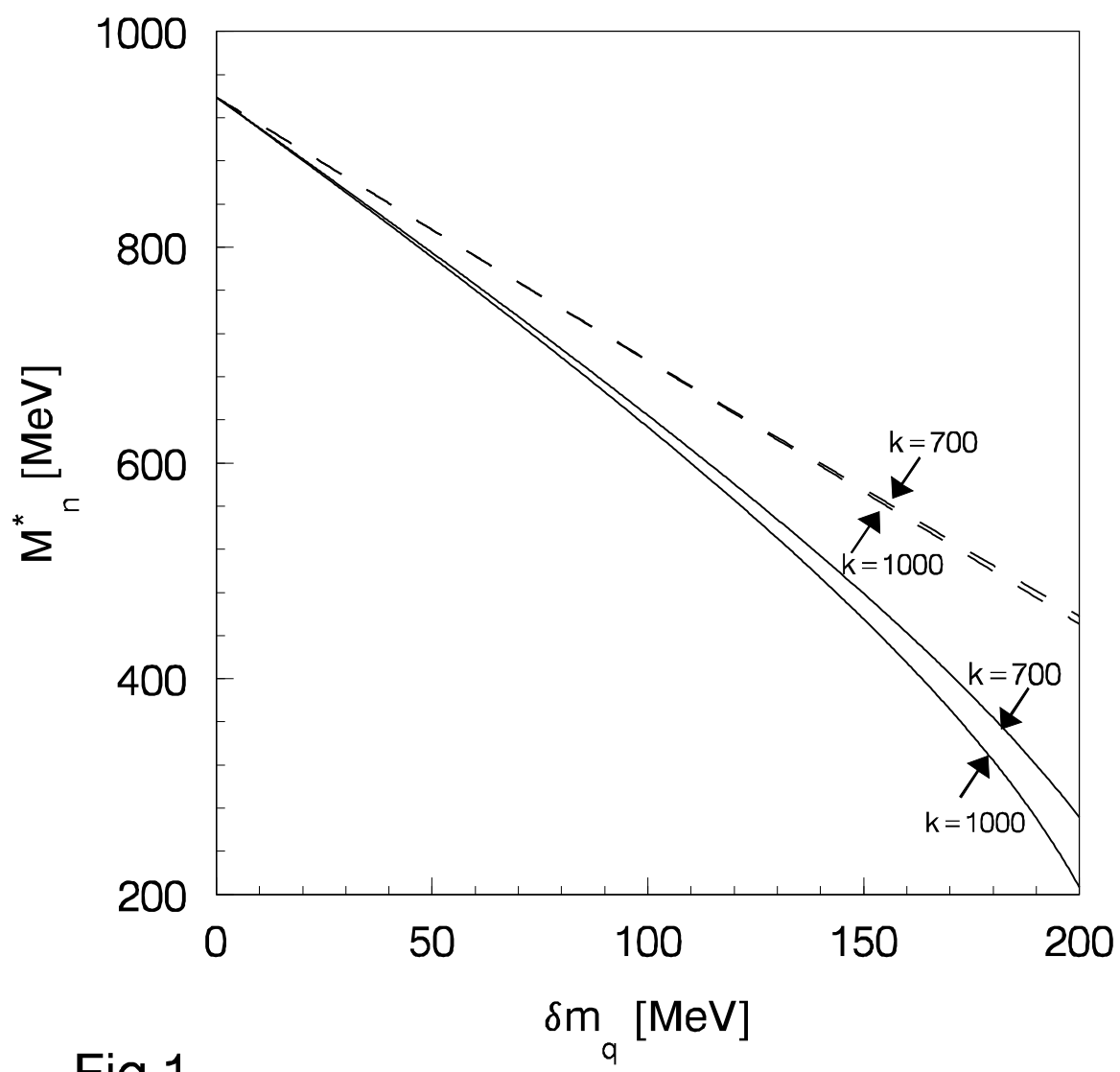


Fig.1

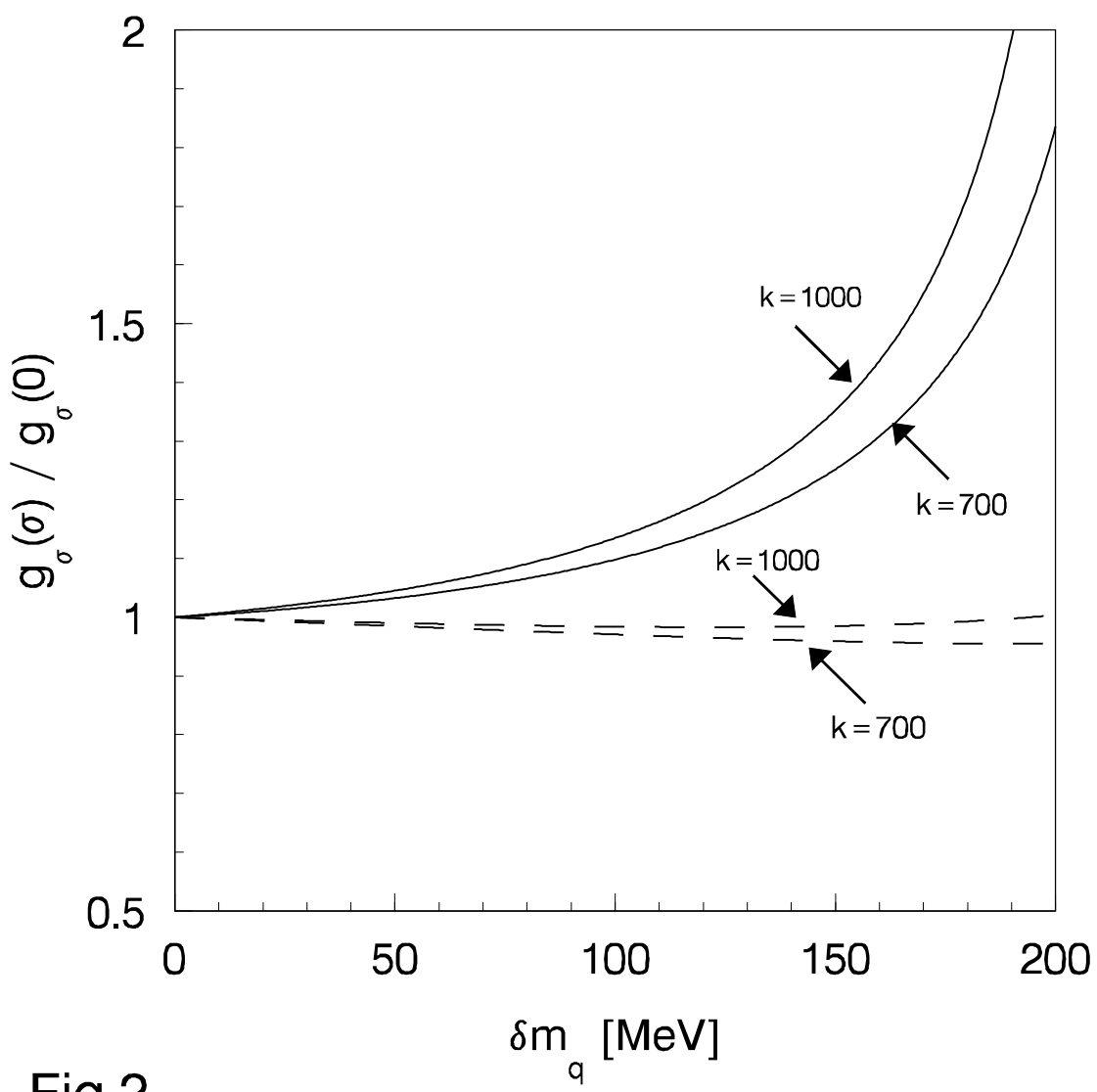


Fig.2

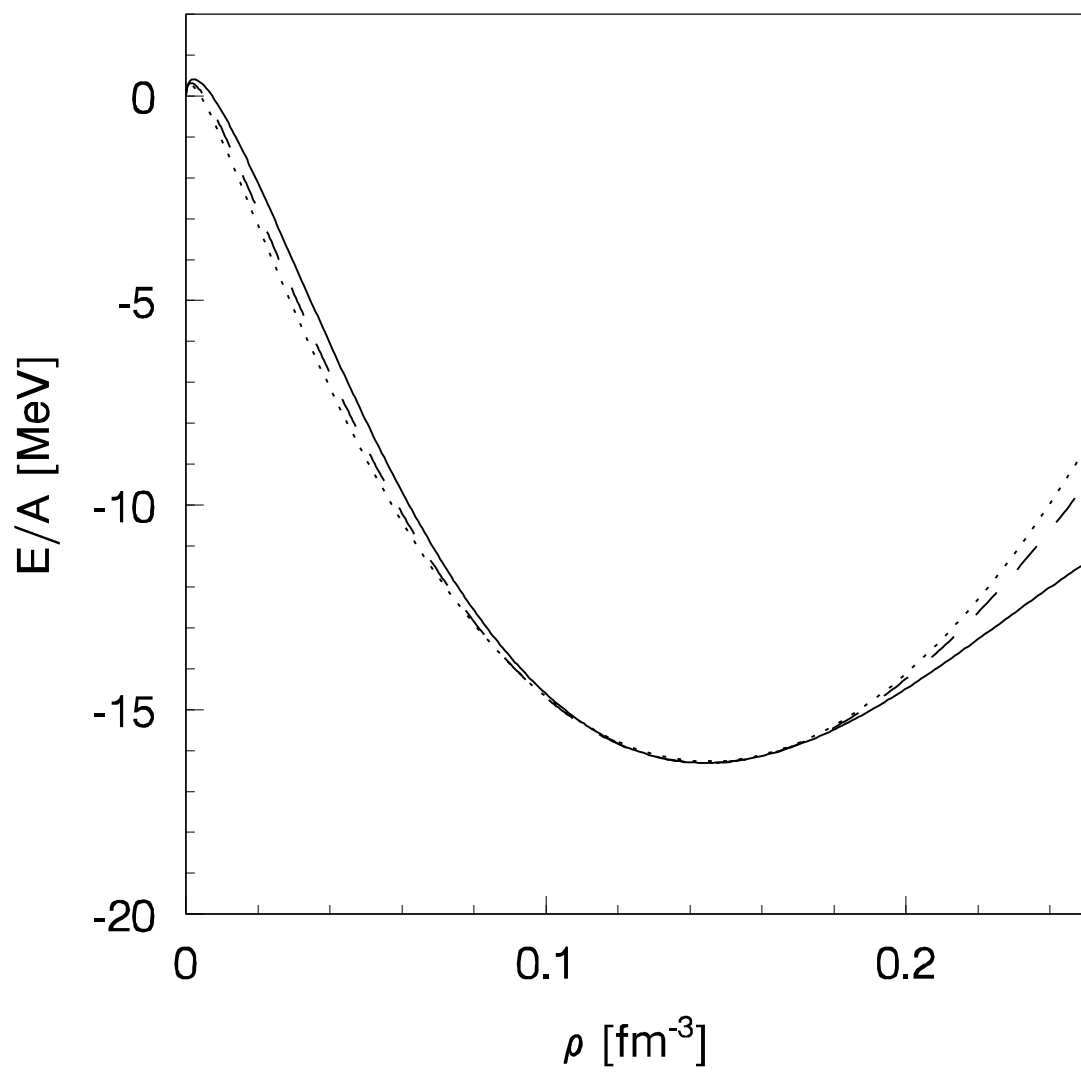


Fig.3

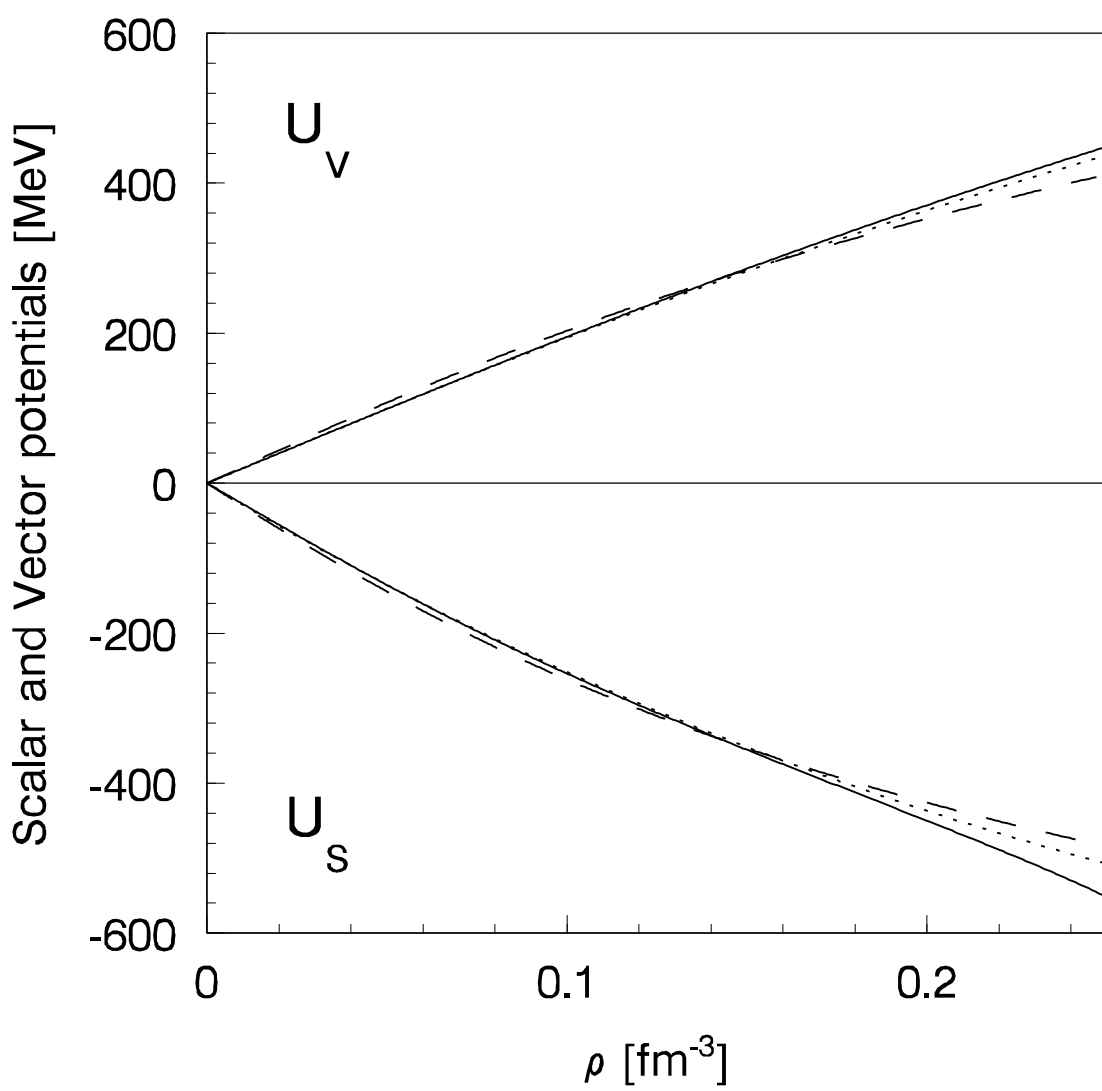


Fig.4

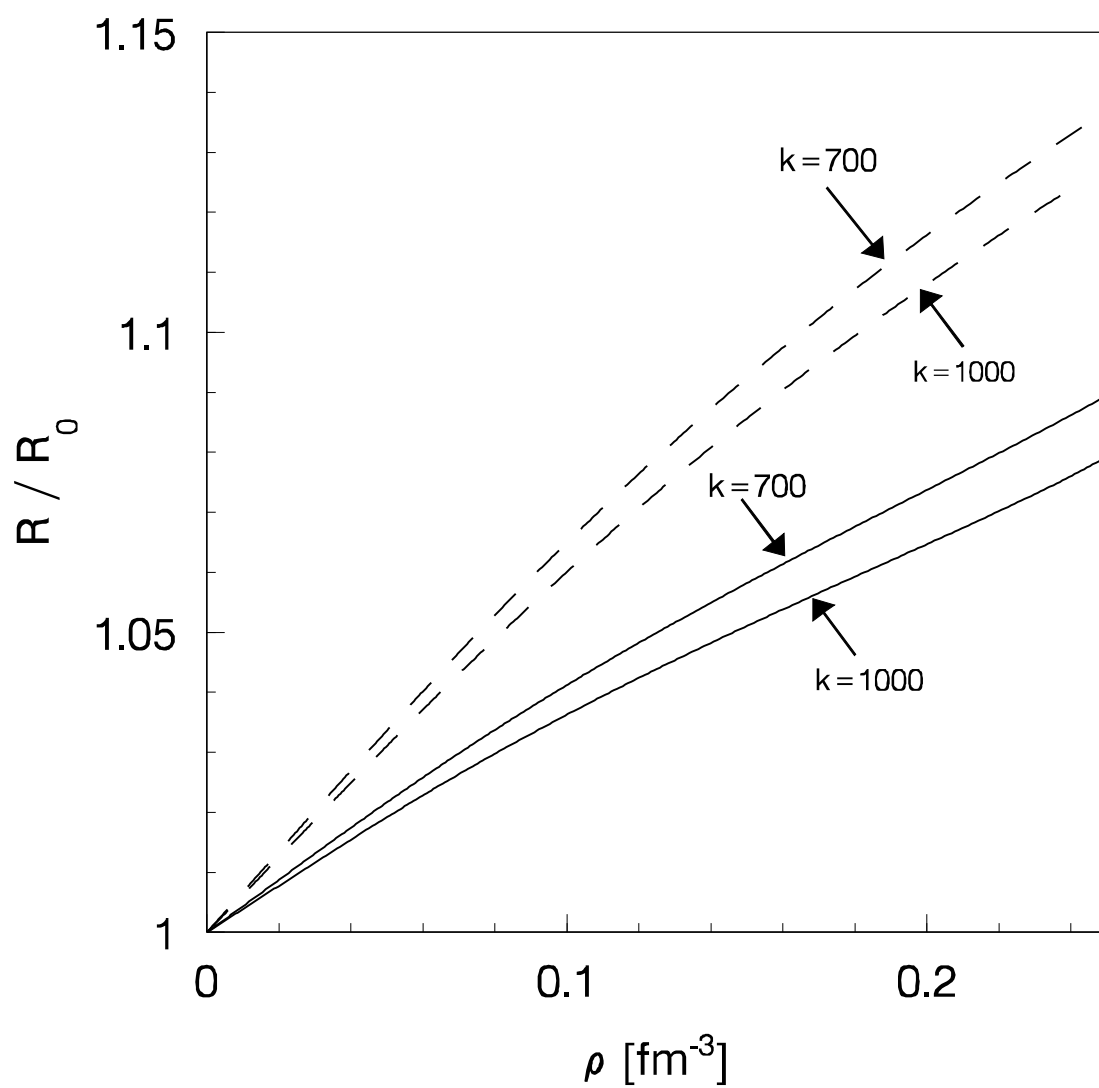


Fig.5

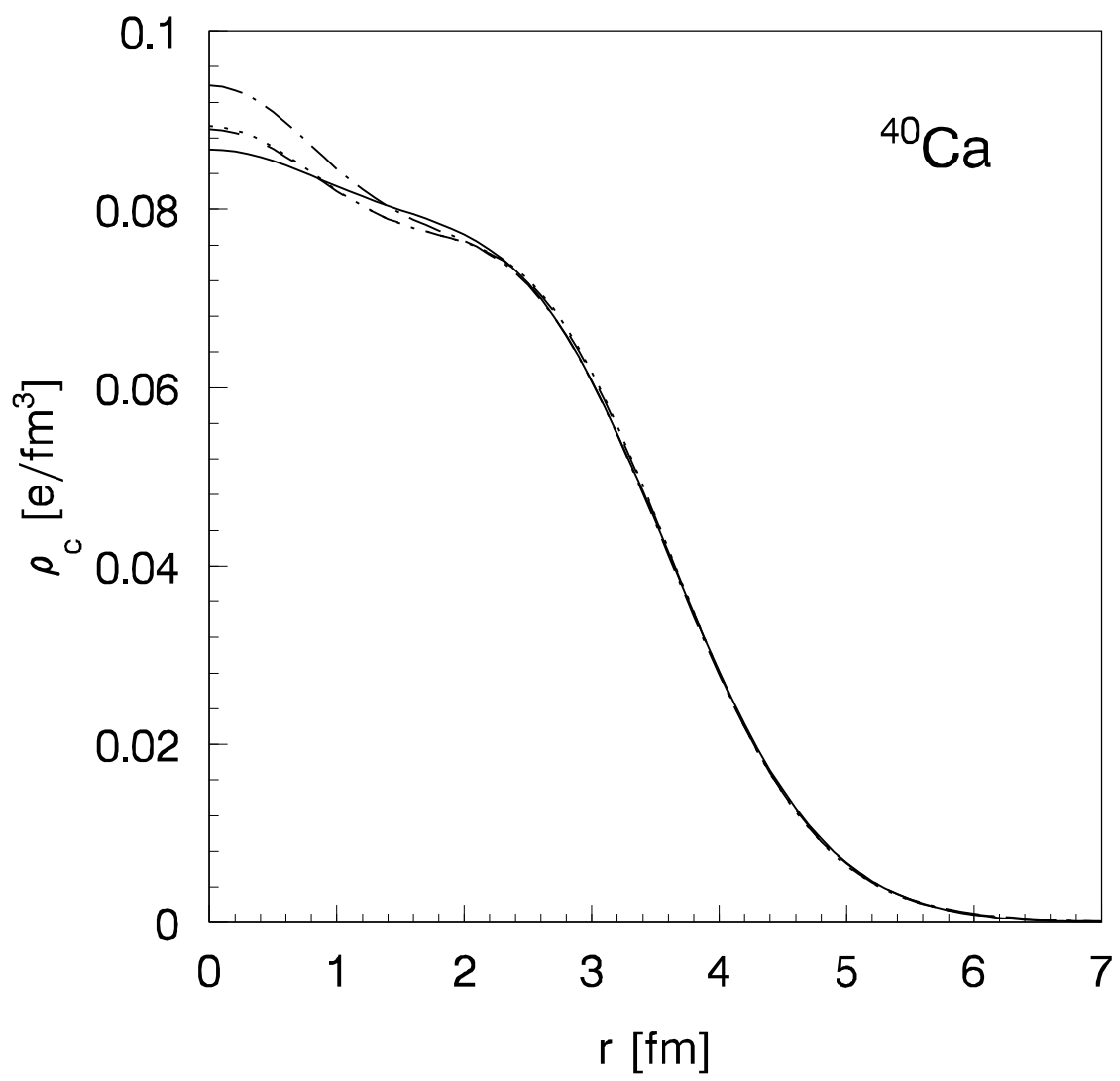


Fig.6